Paper 3

Transient Diffraction Effects in Ultrasonic Meters for Volumetric, Mass and Energy Flow Measurement of Natural gas

Per Lunde, Kjell Eivind Frøysa, Remi A. Kippersrud,
Christian Michelsens Research, Norway and
Magne Vestrheim, University of Bergen, Norway

21st International North Sea Flow Measurement Workshop
Tønsberg, Norway, 28 - 31 October 2002

TRANSIENT DIFFRACTION EFFECTS IN ULTRASONIC METERS FOR VOLUMETRIC, MASS AND ENERGY FLOW MEASUREMENT OF NATURAL GAS

Per Lunde, Christian Michelsen Research AS (CMR), Bergen, Norway
Kjell-Eivind Frøysa, Christian Michelsen Research AS (CMR), Bergen, Norway
Remi A. Kippersund, Christian Michelsen Research AS (CMR), Bergen, Norway
Magne Vestrheim, University of Bergen (UoB), Dept. of Physics, Bergen, Norway

SUMMARY

The influences of transducer diffraction effects on measured USM transit times are investigated, in relation to "dry calibration" methods and consequences for the USM measurement accuracy in flow calibration and field operation. Diffraction effects depend on a number of operational factors. The magnitude of such systematic effects is evaluated using a plane piston model and finite element modelling of the vibration and radiation of typical USM piezoelectric transducers. Consequences for volumetric, mass and energy flow measurement using USMs are evaluated. In a cooperation with industry partners, data from flow calibration of a USM are used to illustrate the significance and potentials of improved control with diffraction effects. It is shown that especially for small-size meters (4"-12") treatment of diffraction effects is highly recommended if high accuracy of the volumetric flow rate measurement is needed, and if the USM is used as a mass or energy flow meter. For the VOS measurement used in mass and energy flow metering, flow calibration does not reduce the error due to diffraction, whereas for the volumetric flow measurement, this error can be reduced by flow calibration. Methods to achieve improved control with diffraction effects are described.

1. INTRODUCTION

In custody transfer metering of gas, multipath ultrasonic transit-time flow meters (USM) are being used for volumetric flow rate measurement [1,2]. In addition to the flow velocity and volumetric flow rate, USMs can also give measurements of the velocity of sound (VOS) in the gas. The VOS measurement has traditionally been used for self diagnostics of the USM [3].

There is today an increasing interest in exploiting the potentials of USMs for extended applications, such as direct mass and energy measurement, using the volumetric flow rate measurement in combination with the VOS measurement, as an additional output from such meters. Developments in recent years have resulted in methods for calculating the density [4-14] as well as the calorific value [13-22], from the measured VOS in the gas.

The accuracy of such density and calorific value measurements depend on several factors, - one major factor being the accuracy of the VOS measurement, which should be ±0.3 m/s (about ±0.075 %) or better (standard uncertainty) [14]. Among others this puts requirements on improved control of transit time measurements in the USM, such as systematic effects due to e.g. (a) transducer time delay correction ("dry calibration" values), (b) time delay due to transducer diffraction effects, (c) variation of these corrections with pressure, temperature, path length and gas composition, (d) sound refraction (flow profile effects on transit times), (e) finite beam effects, and (f) cavity flow effects. These effects are accounted for by different methods and to varying degree in today's USMs.

In the present work the influences of transducer diffraction effects on measured USM transit times are investigated in relation to the USM measurement accuracy. Transducer diffraction effects depend on a

number of factors, such as pressure, temperature, path length, VOS (gas composition), transducer diameter, operational frequency, transducer vibration pattern (displacement), transducer bandwidth, time detection method, etc. Earlier works in this field [23-29] have employed simplified models for description of diffraction correction. The present work extends these earlier works by using finite element modelling of typical USM piezoelectric transducers to evaluate the magnitude of such diffraction effects, as well as by evaluating consequences for flow calibration and field operation of USMs in relation to the use of actual “dry calibration" methods.

Most current USMs apply time detection in the start of the acoustic signal, i.e. in the socalled transient part of the signal. Since transducer diffraction effects depend on whether time detection is made in the transient (start) or in the stationary (middle) part of the signal, both cases are addressed here. Consequences for volumetric, mass and energy flow measurement using USMs are evaluated. In a cooperation with industry partners, data from flow calibration of a USM are used to illustrate the significance and potentials of control over such transducer diffraction effects.

In perspective, it is important to be aware that the results presented here do not question the basic soundness and reliability of the USM method. The diffraction effects discussed here become important essentially when (a) high accuracy in the volumetric flow rate reading is necessary, and (b) for extended functionality of USMs (use of the measured VOS to calculate the mass and energy flow rates). Control of diffraction effects become especially important for the VOS measurement, for which possible systematic effects (errors) are *not* being eliminated or reduced by flow calibrating the meter. The primary intention of the present work is to provide a basis to further improve today’s USM technology towards higher accuracy, control, reliability and functionality.

2. PROBLEM DESCRIPTION

The present work addresses consequences of transducer diffraction effects in flow calibration and field operation of USMs, given that a “dry calibration” [1] of the USM has already been performed. Such consequences will depend on which “dry calibration” method that has been used. Thus, as a basis for the discussion, the present section summarizes briefly the basic USM relationships needed in the discussion, various relevant “dry calibration” methods, as well as strategies used here for description of diffraction effects.

2.1 Basic relationships and time delay correction

In ultrasonic transit time flow metering of gas the volumetric flow rate and the velocity of sound (VOS) are given (in units of [m^3/s] and [m/s]) as [27,30-33]

$$q_{USM} = 2\pi R^2 \sum_{i=1}^{N} w_i \frac{(N_{refl,i}+1)\sqrt{R^2 - y_i^2}\,(t_{1i} - t_{2i})}{t_{1i} t_{2i} \left| \sin 2\phi_i \right|} \quad , \tag{1a}$$

$$c_i = \frac{L_i \sqrt{(t_{1i} + t_{2i})^2 \cos^2 \phi_i + (t_{1i} - t_{2i})^2 \sin^2 \phi_i}}{2 t_{1i} t_{2i} \cos \phi_i} \quad , \tag{1b}$$

where (cf. Fig. 1)

N: number of acoustic paths,
R: inner radius of the USM meter body,
y_i: lateral distance from the pipe center (lateral chord position) for path no. i, $i = 1, \ldots, N$,
L_i: interrogation length for path no. i, $i = 1, \ldots, N$,
ϕ_i: inclination angle (relative to the pipe axis) of path no. i, $i = 1, \ldots, N$,
w_i: integration weight factor for path no. i, $i = 1, \ldots, N$,

t_{1i}: plane wave transit time for upstream sound propagation of path no. i, $i = 1, \ldots, N$,
t_{2i}: plane wave transit time for downstream sound propagation of path no. i, $i = 1, \ldots, N$,
$N_{refl,i}$: number of wall reflections for path no. i, $i = 1, \ldots, N$ ($N_{refl,i} = 0$, 1 or 2 in current USMs),
c_i: velocity of sound (VOS) for path no. i, $i = 1, \ldots, N$.

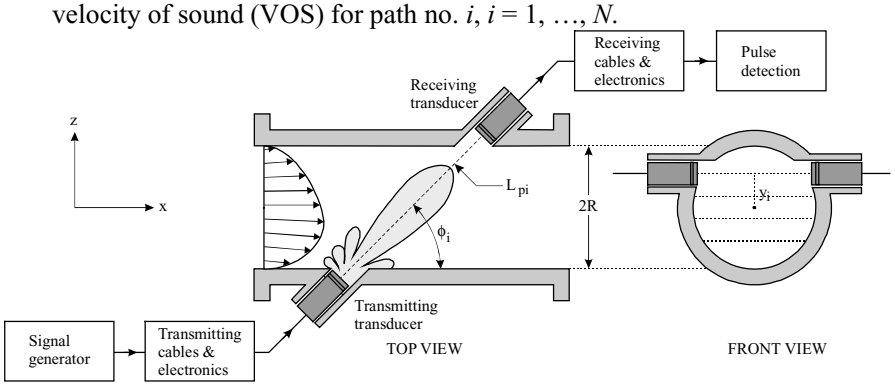

Fig. 1. Schematic illustration of a single path in a multipath ultrasonic transit time flow meter with non-reflecting paths (for downstream sound propagation). (Left: centre path example ($y_i = 0$); Right: path at lateral chord position y_i.)

The accuracy of such measurement depends on a number of factors (cf. e.g. [27-31]), - one major factor being the accuracy of the transit time measurements in the USM.

The measured transit times can formally be "decomposed" into systematic terms and random terms. Random terms are due to e.g. turbulent temperature and velocity fluctuations in the flow, incoherent noise (RFI, pressure control valves, pipe vibrations), coherent noise (acoustic cross-talk through meter body, electromagnetic cross-talk, acoustic reverberation in gas), finite clock resolution, electronics stability (possible random effects), possible random effects in signal detection/processing (e.g. erroneous signal period identification), and power supply variations [30,31].

Systematic contributions to the measured transit times are e.g. (for each path in the USM) [30,31]

- time delay due to electromagnetic wave propagation in electronics and cables,
- time delay due to elastic wave propagation in the piezoelectric transducers (transducer time delay),
- time delay due to sound propagation in the two transducer port cavities,
- "time delay" (travel time) due to sound propagation in the flowing fluid (within the pipe bore),
- time delay due to diffraction effects at transducers (diffraction time delay),
- difference between measured upstream and downstream transit times at zero flow ("Δt-correction"),
- possible deposits at transducer front (lubricant oil, liquid, wax, grease, etc.),
- possible systematic effects in signal detection/processing (e.g. erroneous signal period identification),
- sound refraction (flow profile effects on transit times), and
- possible beam reflection at the meter body wall (for reflecting-path meters).

The "time delay" due to sound propagation in the flowing fluid (within the pipe bore) is normally assumed to correspond to plane-wave propagation of the sound pressure signal over the interrogation length [27]. This "time delay" is then taken to be the transit time to be used in Eqs. (1). Other time delays have to be corrected for in the USM software, if possible.

Such time corrections have been realised or implemented in different ways by the different USM manufacturers. One possible way of expressing the time corrections is [27]

$$t_{1i} = t_{1i}^{measured} - t_{1i,0}^{cab,el,tr} - t_{i,0}^{dif} - t_i^{cavity} \tag{2a}$$

$$t_{2i} = t_{2i}^{measured} - t_{1i,0}^{cab,el,tr} - t_{i,0}^{dif} + \Delta t_{i,0}^{corr} - t_i^{cavity} \tag{2b}$$

where

$t_{1i}^{measured}$, $t_{2i}^{measured}$:	Measured upstream and downstream transit times of path no. *i*,
$t_{1i,0}^{cab,el,tr}$:	Time delay due to cables, electronics and transducers (transmit and receive), for upstream propagation of path no. *i*, at "dry calibration" conditions (usually measured),
$\Delta t_{i,0}^{corr}$:	Δt-correction of path no. *i*, at "dry calibration" conditions (usually measured, or reduced (and in some cases practically eliminated) by reciprocal design of the electroacoustic system),
$t_{i,0}^{dif}$:	Upstream and downstream diffraction time delay of path no. *i*, at "dry calibration" conditions (usually calculated),
t_i^{cavity} :	time delay due to sound propagation in the two transducer port cavities, for path no. *i* (calculated).

2.2 Review of current "dry calibration" strategies in relation to treatment of diffraction effects

To have confidence in a particular meter at hand, it is general practice to carry out a "zero-flow verification" of the meter, i.e. a best possible zero flow reading at "zero flow". For example, the AGA-9 report concerned with gas meters [1] recommends that the zero flow reading should be less than 0.04 ft/s = 12.2 mm/s for each path.

To enable sufficient zero-flow verification, geometrical quantities and time delays addressed above are measured for the meter at hand in a "dry calibration" procedure [1, p. C-31]. Time delays can be measured for a specific set of electronics, cables and transducers, for a single pressure-temperature point, or several points. Different "dry calibration" strategies may be used. To illustrate typical challenges that may arise in connection with use of such strategies, some "dry calibration" methods involving dedicated test cells (without fluid flow) are briefly addressed in the following.

1. ***Sound velocity method***. One "dry calibration" method summarized in the AGA-9 report [1, p. C-31] is to determine the time delay at each path from the difference between measured and calculated transit times, using two transducers at a known separation distance, at zero flow. The calculated transit time is obtained as the ratio of the transducer separation distance to the sound velocity in the test fluid. Both need to be known very accurately.

   For instance, for a 6" gas meter, the corresponding requirement to the total time delay is about 400 ns to keep the USM flow velocity error less than 0.2 % in a metering situation (isolated contributions from time delay error only). This number results from an analysis of the integrated error effect in a flow meter, by increasing all transit times in Eq. (1a) by 400 ns. Consequently, the VOS in "dry calibration" needs to be known better than about 0.5 m/s when "dry calibration" is made at a transducer distance of 10 cm, 0.16 m/s at a distance of 30 cm, and 0.05 m/s at a distance of 100 cm (provided nitrogen is used as "dry calibration" gas). This corresponds to a temperature control of 0.8 °C, 0.3 °C and 0.08 °C, for the three example distances, respectively.

For gas meters nitrogen is a common test gas, with well tabulated sound velocity [34]. It is emphasized that good temperature control is essential to keep the sound velocity within these limits.

There is however a problem with this approach. AGA-9 does not discuss diffraction effects, and the method, as stated by AGA-9, does not account for the fact that the diffraction time delay changes with path length [27] cf. e.g. Fig. 7b.

Possible ways to overcome this problem include:

(a) By using the same path lengths (for the "dry calibration" in the cell) as used in the meter, the effect of diffraction correction variation with path length should be insignificant.

(b) Alternatively, if the variation of the diffraction time delay with path length is known, either from measurement or calculation, the time delay can be corrected for this effect.

2. ***Two-distance method***. A second "dry calibration" method which does not require knowledge of the sound velocity in the test fluid has also been summarized in AGA-9 [1, p. C-31]. The time delay at each path can be determined from a setup in which the transit time is measured at two known and different transducer separation distances, at zero flow. The AGA-9 report states that "since the transit time measurements include the same delay time for both path lengths" the time delay can be readily determined.

   There is a problem also with this approach. AGA-9 does not discuss diffraction effects, and the method, as stated by AGA-9, does not account for the fact that the diffraction time delay changes with path length [27], cf. e.g. Fig. 7b. Thus, the two transit time measurements do *not* include the same delay time for the two transducer separation distances, and - depending on the accuracy requirements - the time delay can not be so readily determined.

   In cases for which transducer diffraction effects has significant implications for the USM accuracy, there may be ways to avoid this problem:

   (a) If the diffraction time delay and its variation with distance are known for the transducers in question, either from measurement or calculation, the time delay at each of the two transducer distances can be determined, and the time delay extrapolated to the actual path lengths of the USM.

   (b) Alternatively, by using two transducer separation distances which are both *sufficiently well* into the far field of the transducer, the variation of the diffraction time delay with distance may become insignificant (cf. Fig. 7), and the method described by AGA-9 may be used. An extrapolation of the time delay to the actual path length is in any case needed, however, using e.g. a model for the diffraction correction.

   It is emphasized that good temperature control is essential also in this method, so that the difference in sound velocity between the two measurements becomes insignificant. For instance, the 400 ns requirement in question for a 6" gas meter (see above), corresponds to temperature control better than about 0.4 ^{o}C when "dry calibration" is made at transducer distances of 10 and 20 cm, and better than 0.06 °C when transducer distances of 60 and 100 cm are used (provided nitrogen is used as "dry calibration" gas).

3. ***Acoustic reflector method***. A third method which does not require knowledge of the sound velocity in the test fluid nor the transducer distance, has been described in [27, p. 49-51]. The time delay due to electronics, cables and transducers at each path can be determined from a setup in which the transit time is measured using a single transducer and an acoustic reflector, at zero flow. The method is an

approximate method, valid under a certain assumption for the diffraction time delay upon reflection at the transducer.

As this method gives the time delay due to electronics, cables and transducers only, the diffraction time delay needs to be determined by other means, either by measurement or calculation.

4. ***Transducer reflection method.*** A fourth "dry calibration" method, which does not require knowledge of the sound velocity in the test fluid nor the transducer separation distance, is also available (not reported in open literature) [35]. The time delay due to electronics, cables and transducers at each path can be determined from a setup in which the transit time is measured using two transducers at a single known distance, at zero flow. The method is an approximate method, valid under certain assumptions for the diffraction time delay upon reflection at the transducers.

   As this method gives the time delay due to electronics, cables and transducers only, the diffraction time delay needs to be determined by other means, either by measurement or calculation.

Consequently, for all of these possible "dry calibration" methods, the diffraction time delay and its variation with distance may need to be known, for the actual transducers used, either by measurement or calculation.

Besides, there adds the complication that the transducer time delay and the diffraction time delay may depend on pressure, temperature, gas composition and flow velocity (beam drift) [27]. This is further commented in Section 5.

2.3 Modelling of transducer diffraction effects

Effects of diffraction using finite sized receivers were observed in early works using ultrasonic methods for measuring the sound velocity and absorption in gases, liquids and solids. A model for including such diffraction effects was given by Williams in 1951 [36]. In this model a circular plane piston is assumed for the source, and an expression was derived for the averaged free field pressure over a receiver surface area equal to that of the source and centred on the sound beam axis. This method and these results have been a basis for including diffraction corrections in later similar measurement problems both for continuous waves (CW) and pulse applications (e.g. [37-50,23-26,29]). Transient diffraction correction effects, which are important in the use of sound pulses in the measurements, have been studied in particular in some more recent works (e.g. [47-50,23-26,29]), and also to some extent related to use in ultrasonic flow metering (e.g. [23-29]). One important limitation in this method of handling diffraction correction effects lies in the assumption of uniform vibrations over the source and receiver transducer surfaces. More accurate diffraction corrections could have been implemented in USMs if the real vibration pattern of the transducers could have been used.

In the present work numerical calculation methods are used to investigate this topic. Two approaches are used:

(a) ***Approach A*****:** A simplified approach based on one-dimensional (1D) description of the piezoelectric transducers (the Mason model) [51], Williams' diffraction correction model for a uniform plane piston mounted in an infinite rigid baffle (for the sound propagation in the gas, see above) [36,52], combined in a system model (*FLOSIM*) [53] to calculate frequency responses, time signals and diffraction time delays. This approach was presented and used in [29].

(b) ***Approach B*****:** A recently developed approach based on finite element modelling (FEM) of the piezoelectric transducers [54-56] and the resulting sound propagation in the fluid (gas). The *FLOSIM*

system model has been further developed to include the FEM results in the calculation of frequency responses, time signals and diffraction time delays. This approach was presented in [57].

Emphasis is here laid on the influences of path length, transducer bandwidth, actual transducer vibration, and where in the signal the time detection is made (transient part, or stationary part), as well as consequences for the USM measurement accuracy. Pressure, temperature, gas composition and beam drift effects on diffraction time delay are not addressed in detail here.

3. THEORY

The present section describes the methods used to calculate the diffraction time delay for the transient and stationary parts of the acoustic signal.

3.1 Representation of transducer diffraction effects in USM measurement systems

The geometry used for this problem is shown in Fig. 2. Note that the description used here represents a simplification relative to the more realistic situation illustrated in Fig. 1, so that e.g. effects of transducer port cavities are not accounted for.

The diffraction time delay is defined as the time shift of the acoustic signal in the fluid, relative to a plane wave, due to acoustic diffraction at the receiving transducer (i.e. that the wave fronts are not plane). More precisely; the time shift from the plane-wave sound pressure in the fluid at the centre point of the receiving transducer front (in absence of the receiving transducer) -to- the free-field sound pressure in the fluid, integrated over a circular "measurement area" corresponding to the receiving transducer front (in absence of the receiving transducer) [42,43].

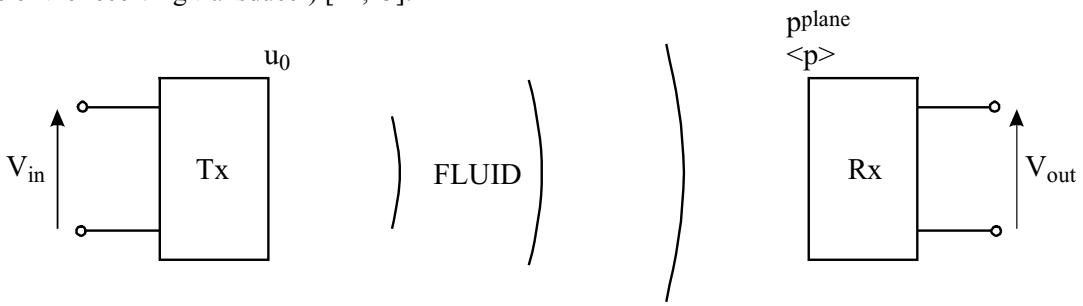

Fig. 2. Geometry and symbols used to describe diffraction correction in a a single path of a multipath ultrasonic transit time flow meter with non-reflecting paths.

To see how diffraction effects influence on the measured acoustic signals (such as the transit times), consider two different transfer function models for sound propagation from transducer Tx to transducer Rx in path no. *i*. These are the plane wave propagation model and a relatively general propagation model, given as[1]

$$\frac{V_{out}^{plane}}{V_{in}} = \frac{u_0}{V_{in}} \frac{p^{plane}}{u_0} \frac{V_{out}^{plane}}{p^{plane}} \tag{3a}$$

$$\frac{V_{out}}{V_{in}} = \frac{u_0^{eq,pist}}{V_{in}} \frac{p^{eq,plane}}{u_0^{eq,pist}} \frac{\langle p \rangle}{p^{eq,plane}} \frac{V_{out}}{\langle p \rangle} \quad , \tag{3b}$$

respectively, where

[1] For USMs applying current signal output of the receiving transducer, the present theory can be applied by terminating the receiving transducer in a low electrical impedance (e.g. 1 Ω), cf. Fig. 3.

V_{in}: Input voltage to the transmitting transducer Tx,

V_{out}^{plane}: Output voltage from the receiving transducer Rx, for the plane wave sound propagation model and the electrical termination at hand,

V_{out}: Output voltage from the receiving transducer Rx, for the general sound propagation model and the electrical termination at hand,

u_0: Volume velocity at the front surface of the transmitting transducer Tx, for the plane wave sound propagation model,

$u_0^{eq,pist}$: Equivalent volume velocity at the front surface of the transmitting transducer Tx, for the general propagation model (extrapolated from the farfield using the piston model),

p^{plane}: Plane-wave sound pressure in the fluid at the centre point of the receiving transducer front (in absence of the receiving transducer),

$p^{eq,plane}$: Equivalent plane-wave sound pressure in the fluid at the centre point of the receiving transducer front (in absence of the receiving transducer), for the general sound propagation model,

$\langle p \rangle$: free-field sound pressure in the fluid, integrated over a circular "measurement area" corresponding to the receiving transducer front (in absence of the receiving transducer).

As Eqs. (3) represent frequency domain descriptions (transfer functions), all quantities are functions of frequency. They represent convenient ways of "decomposing" the plane wave field and the general sound field into transfer functions, such as e.g. to describe effects of diffraction on the sound propagation.

The plane wave model in Eq. (3a) serves as a reference model only, and can not give a correct description of real sound fields. Eq. (3b) is chosen to better represent real (measured or simulated) sound fields, for reasons as described in the following. At very long ranges (farfield), nearfield effects due to diffraction are absent. Thus, by extrapolating the observed (measured or simulated) farfield on-axis sound pressure back to the transducer surface using the plane piston model (cf. Section 3.3), diffraction effects are "assembled" into the transfer function $\langle p \rangle / p^{eq,plane}$. As a consequence, the real sound field will in this model coincide with the (hypothetical) plane piston sound field in the farfield, on the acoustical axis, but not off-axis, and not in the nearfield.

In Eqs. (3), u_0 / V_{in} and $u_0^{eq,pist} / V_{in}$ are the transfer functions of the transmitting transducer, in the plane wave and general sound propagation models, respectively. The plane wave sound propagation in the fluid is given as

$$\frac{p^{plane}}{u_0} = \frac{p^{eq,plane}}{u_0^{eq,pist}} = \frac{\rho c}{A} e^{-ikz} \quad , \tag{4}$$

where ρ and c are the fluid density and sound velocity (VOS), respectively, A is the area of the front surface of the transmitting transducer, z is the axial distance between the transducers, $k = \omega / c$ is the acoustic wavenumber, $\omega = 2\pi f$ is the angular frequency, and f is the frequency. $\langle p \rangle / p^{plane}$ is per definition the diffraction correction [42,43],

$$H^{dif} \equiv \frac{\langle p \rangle}{p^{eq,plane}} \quad . \tag{5}$$

Now, assume the simplification that the transfer function $V_{out}/\langle p \rangle$ of the receiving transducer is independent of axial distance between the two transducers (i.e. whether the receiver is in the near field, the intermediate region or in the far field), so that

$$\frac{V_{out}}{\langle p \rangle} = \frac{V_{out}^{plane}}{p^{plane}} = \frac{V_{out}^{ff}}{p^{ff}} \quad , \tag{6}$$

where

p^{ff} : Axial sound pressure in the far field of the transmitting transducer,

V_{out}^{ff} : Output voltage from the receiving transducer Rx, in the far field, and for the electrical termination at hand.

The term V_{out}^{ff}/p^{ff} is of interest here since this is an expression conveniently used for calculating the transfer function of the receiving transducer (cf. e.g. [51,57]).

From Eqs. (3)-(6) one finds that the plane wave propagation model and the full propagation model become

$$\frac{V_{out}^{plane}}{V_{in}} = \frac{u_0}{V_{in}} \frac{\rho c}{A} e^{-ikz} \frac{V_{out}^{ff}}{p^{ff}} \quad , \tag{7a}$$

$$\frac{V_{out}}{V_{in}} = \frac{V_{out}^{plane}}{V_{in}} \frac{u_0^{eq,pist}}{u_0} H^{dif} \quad , \tag{7b}$$

respectively. These are relatively generally valid expressions used in the following.

In the present work two propagation models are used for evaluation of H^{dif}: (a) a simplified approach based on the model for a uniform (plane) piston mounted in an infinite and rigid baffle, and (b) finite element modelling of the piezoelectric transducer at hand and the resulting sound propagation in the fluid medium.

3.2 Approach A for calculation of diffraction correction: Plane piston model

In the first approach, a simplified propagation model is used for evaluation of H^{dif}, namely the model for a circular plane piston mounted in a rigid baffle of infinite extent, given by Willliam's integral expression [35], which can be written as

$$H^{dif} \equiv \frac{\langle p \rangle}{p^{eq,plane}} = 1 - \frac{4}{\pi} \int_0^{\pi/2} e^{ikz\left[1-\sqrt{1+\frac{4a^2}{z^2}\cos^2\theta}\right]} \sin^2\theta d\theta = 1 - \frac{4}{\pi} \int_0^{\pi/2} e^{i\frac{S(ka)^2}{2\pi}\left[1-\sqrt{1+\frac{16\pi^2}{S^2(ka)^2}\cos^2\theta}\right]} \sin^2\theta d\theta \tag{8}$$

where a is the radius of the plane piston (the transducer front surface), the transmitting and receiving transducers have been assumed to have equal radii, S is defined as

$$S \equiv \frac{z}{a^2/\lambda} \quad , \tag{9}$$

and λ is the acoustic wavelength. S is the axial distance z normalized to the last axial pressure maximum in the piston model, a^2/λ.

One should be aware that, although definitely being of substantial value for analysis and treatment of transient diffraction effects in ultrasonic transit time gas flow meters [29]. Approach A is still limited with respect to the description of such effects, e.g. since it does not account for the non-uniform behavior of real transducers. Such behavior is accounted for in Approach B, cf. Section 3.3.

3.3 Approach B for calculation of diffraction correction: Finite element modelling of transducer vibration and radiation

In the second approach, the diffraction correction H^{dif} is calculated for the actual transducer at hand using finite element modelling (FEM) of the piezoelectric transducer [54-57] and the resulting sound field in the fluid (gas).

The FE model used is based on the *FEMP 3.0* model previously developed in a cooperation between CMR and UoB [54-56]. This model can describe effects of different parts in the transducer structure as well as the effects of the resulting vibrations on the radiated sound field, under the assumption of axial symmetry. In addition to being used and tested versus measurement results and numerical accuracy in connection with transducer design and construction, *FEMP* has been further developed such as to describe also the receiving transducer (voltage and current reception), animation of transducer vibration and sound propagation, inclusion of fluid medium losses, adaptation to *FLOSIM* time domain type of modelling, etc. The present code is denoted *FEMP 3.4* [57].

In the present approach, $\langle p \rangle$ is calculated using the FE calculated sound pressure field in the fluid at the receiver position, by averaging over the receiver surface area. The corresponding equivalent plane wave sound pressure at the receiver position, $p^{eq,plane}$, is calculated from the farfield FE calculations as follows: Let z_{ff} be an axial distance *well* into the farfield of the transducer (in practice, and somewhat arbitrarily, we have used z_{ff} = 1000 m), and let p_{ff} denote the FE calculated sound pressure at z_{ff}. Firstly, the "equivalent piston volume velocity" is calculated by extrapolating this farfield pressure back to the surface of a hypothetical "equivalent plane piston", located at the position of the transducer front surface, using the farfield expression for the sound field radiated by a uniform piston in a rigid baffle [52]. This "equivalent piston volume velocity" is given as

$$u_0^{eq,pist} = p_{ff} \frac{z}{i\rho f} e^{ikz_{ff}} \quad . \tag{10}$$

The equivalent plane wave sound pressure $p^{eq,plane}$ is then calculated at the receiver position using Eq. (4). Finally, H^{dif} is calculated from Eq. (5). This procedure is used for each frequency.

3.4 Factors influencing on diffraction correction

From Eq. (9) it appears that in the plane piston model, the diffraction correction H^{dif} depends on two key parameters, S and ka, which again depend on several more basic parameters, such as

- the transducer distance, z,
- the fluid sound velocity, c,
- the frequency, f, and
- the radius of the plane piston, a.

In addition, the diffraction correction depends on

- where in the signal time detection is being made (transient part, or stationary part),

- the frequency response and bandwidth of the acoustic transmit - receive system.

In addition, real transducers do very seldom vibrate as a plane piston, so in practice diffraction correction will also depend on

- the vibration pattern (vibration modes and "shape") of the transducer at hand, i.e. the actual directivity of the transducer (magnitude and phase).

Normally, factors such as bandwidth, vibration pattern and directivity will vary with the temperature T, and possibly also with pressure P in the gas. This is so especially if polymer or epoxy materials are involved in the transducer construction, which is very often the case in actual USM transducers used for gas. If so, the diffraction correction H^{dif} will also depend on T and P [27].

3.5 Calculation of diffraction time delay for transient signals

Calculation of diffraction time delay for transient signals has been made using the *FLOSIM* model for simulation of electro-acoustic measurement systems (in the time and frequency domains), such as a single path in a USM [53,51,23,26,57], cf. Figs. 1 and 3.

In Approach A a one-dimensional (1D) Mason type of model for thickness vibration mode transducers has been used for the transmitting and receiving transducers [51], combined with two models for sound propagation in the fluid: (a) the plane wave model V_{out}^{plane} given by Eq. (7a), and (b) the plane piston model V_{out} given by Eqs. (7b) and (8). With respect to expressions for the transfer functions of the transmitting and receiving transducers, u_0 / V_{in} and V_{out}^{ff} / p^{ff}, respectively, it is referred to [53] and [51]. In Approach B, the *FEMP* finite element model can be used for the transmitting and receiving transducers as well as the sound propagation in the fluid [57].

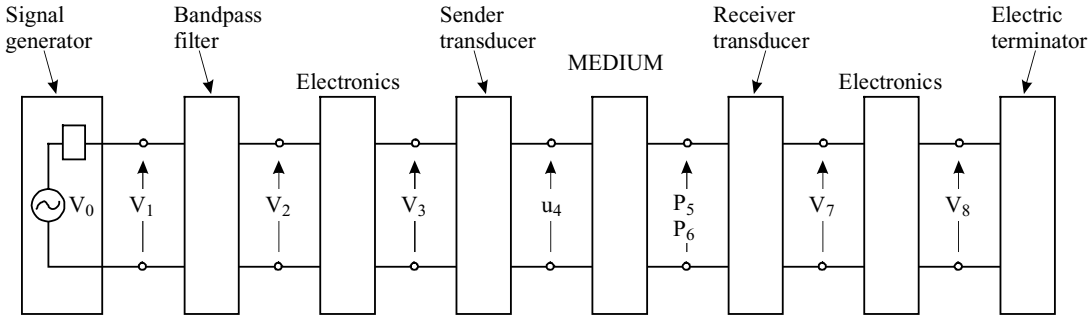

Fig. 3. Schematic overview of the mudule-based *FLOSIM* numerical simulation model for time and frequency domain modelling of an acoustic measurement system, including a single path in a USM [53,51]. Symbols: V is voltage, P is pressure, and u is volume velocity. Subscripts represent node numbers in the model, at which signals and spectra can be calculated.

4. RESULTS - GAS USMS

Diffraction time delay results related to USMs designed for measurement of natural gas are discussed in the following.

4.1 Calculation example

A natural gas at a pressure of about 25 bar is considered here as an example, with density and sound velocity of, say, $\rho = 20$ kg/m^3 and c = 400 m/s. Typically, gas USMs operate at a frequency in the range 100 - 200 kHz, and a signal frequency of 150 kHz is used here as a representative example.

Fig. 4a shows a simplified transducer construction as an example, consisting of a piezoelectric element with a front layer and a backing layer. A 12 x 3 mm lead zirconate titanate type of piezoelectric element is used here (Pz27 [58]), chosen so to operate in its fundamental radial mode at 150 kHz.

The 12 x 4 mm front layer (quarter wavelength thick at 150 kHz, used for impedance matching to the gas) was modelled using a density of 1100 kg/m^3, compressional wave velocity of 2500 m/s, Poisson's ratio of 0.31, and compressional and shear Q factors of 20. The 12 x 18 mm tungsten/araldite backing (used for increasing the transducer bandwidth) was modelled using a density of 10000 kg/m^3, compressional wave velocity of 1600 m/s, Poisson's ratio of 0.2, and compressional and shear Q factors of 5.

By intention, the transducer construction used here as an example may not be quite similar to actual gas USM transducers. However, for the topic of diffraction correction under discussion here, the transducer example is considered to be sufficiently representative.

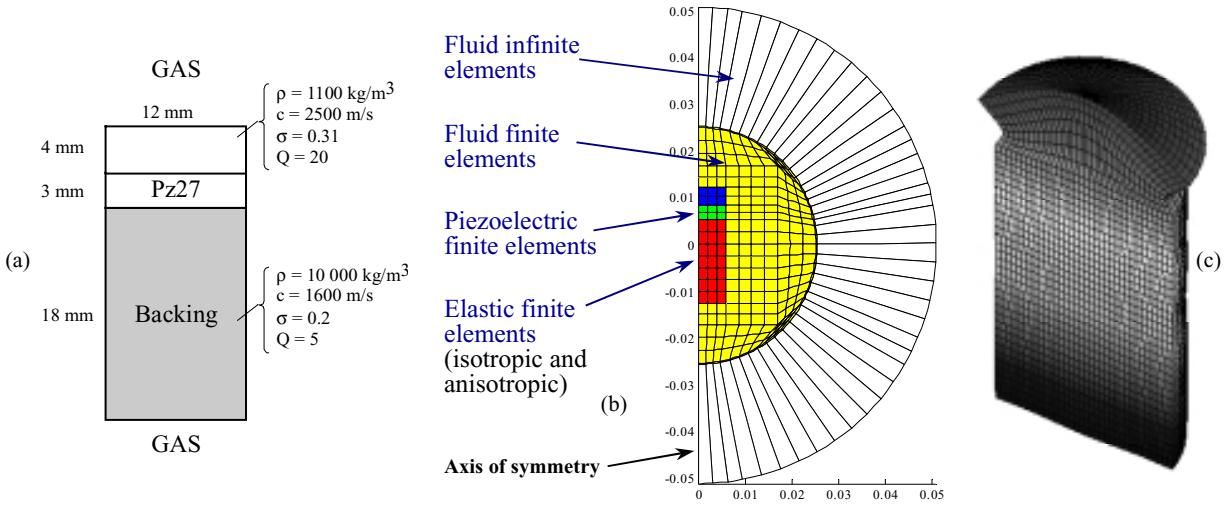

Fig. 4. (a) Transducer example used for simulating properties of a gas USM, (b) simplified numerical grid used for the finite element calculations of the transducer and the radiated sound field, and (c) calculated vibration of the transducer structure at 150 kHz (displacement amplitudes exaggerated $0.5 \cdot 10^6$ times).

Fig. 4b illustrates the finite element mesh used for the modelling of this example transducer structure. Infinite elements are used for the outermost radiated field, beyond 2.5 cm. For clarity, only a reduced mesh consisting of 292 elements is shown in Fig. 4b. (The results given in Figs. 5-8 have been calculated using a mesh of 16736 8-node isoparametric finite elements.)

The calculated vibration pattern (displacement) of the transducer structure is shown in Fig. 4c, at 150 kHz (i.e. at the operational frequency, close to the fundamental radial mode of the piezoelectric element). Note the relatively large and non-uniform displacement amplitude of the front layer relative to the piezoelectric element, which is the active unit exciting the vibration. The actual vibration pattern of the transducer influences on the diffraction correction.

The calculated wave field radiated by this transducer at 150 kHz is shown in Fig. 5c, together with the transducer's vibration pattern. Fig. 5d shows the radiated field for the simplified (and idealized) case of a uniform plane piston mounted in an infinite rigid baffle, with the same diameter as the transducer, 12 mm. The volume velocity of the piston vibration is calculated from the transducer farfield as described in

Section 3.3, i.e. as the "equivalent piston volume velocity", $u_0^{eq,pist}$, given by Eq. (10). Only the nearfield radiations are shown in Figs. 5c and 5d.

The corresponding farfield directivity patterns are shown in Fig. 5a and 5b, at the same frequency, for the "real" transducer vibration, and for the simplified case of a uniform piston vibrating in an infinite rigid baffle, respectively.

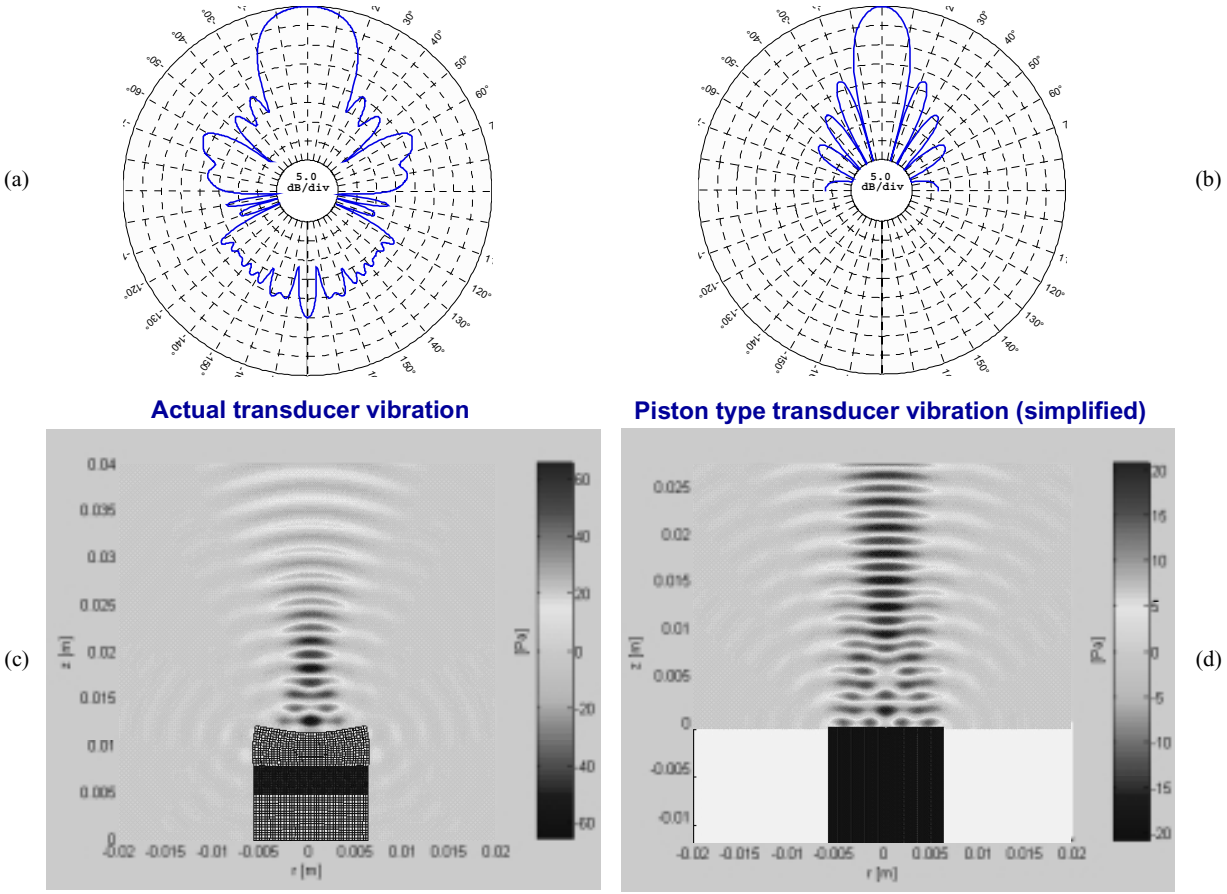

Fig. 5. FE calculated transducer vibrations and radiation at 150 kHz. (a) and (c): the transducer shown in Fig. 4a and c. (b) and (d): uniform plane piston with diameter 12 mm mounted in an infinite rigid baffle. (a) and (b): farfield directivity (at 1 m. distance). (c) and (d): nearfield radiation (with transducer displacement amplitudes exaggerated 10^5 times).

Significant differences are noticed in the sound fields radiated by the plane piston and the transducer. The transducer's nearfield (the region of nearly plane wave propagation) is shorter than the piston's nearfield, so that the transition from nearly plane wave to spherical wave propagation appears at a shorter range for the transducer than for the plane piston (at about 6 mm and 14 mm ranges, respectively). The reason for that is the "bowl-like" vibration of the transducer front, with large amplitude in the centre, decreasing towards the edge. This means that a certain amount of phase shift due to diffraction will be obtained at a shorter range for the transducer than for the plane piston (cf. also Fig. 7a). In other words, at short ranges the diffraction time delay effect is larger for the transducer than for the piston.

In the farfield, the transducer example is much less directive than the piston, cf. Figs. 5a and b. The reason for that is again the "bowl-like" vibration of the transducer front, cf. Figs 4c and 5c. It is important to be aware that Figs. 5a and c demonstrates how this transducer vibrates and radiates at 150 kHz only. At other frequencies, the vibration and radiation are different (not shown here). In practice, the vibration

pattern of real transducers are often observed to change over the frequency band near the operational frequency of the USM [27], due to different vibration modes in the transducer structure being excited. This may results in very different sound fields over the frequency band of interest, which has consequences for the frequency spectrum of the diffraction correction, $H^{dif}(f)$, cf. e.g. Fig. 8. This has also consequences for the diffraction time delay in the transient (start) and stationary parts of the signal. Note that such effects of changing transducer vibration pattern and radiated sound field by frequency are not covered by the plane piston model, which vibrates as a plane piston irrespective of frequency, cf. Fig. 5d.

(a)

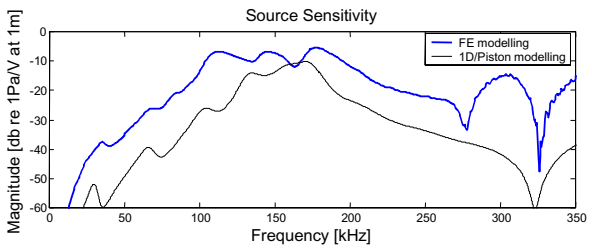

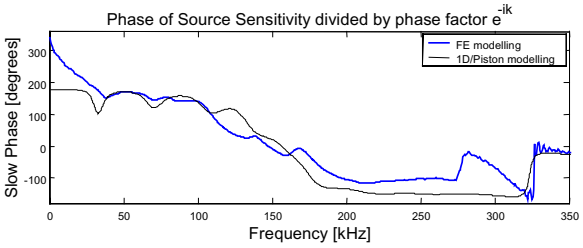

(b)

Fig. 6. Calculated source sensitivity (in natural gas) for the transducer shown in Fig. 4a and c. (a) magnitude and (b) slow phase. *FEMP* calculations (Approach B, blue thick lines) and Mason 1D / piston models (Approach A, black thin lines).

For time detection in the transient part of the signal (e.g. in the first part of the signal), the diffraction time delay depends on the frequency response and bandwidth of the transducer. Fig. 6 shows the calculated magnitude and phase of the voltage source sensitivity (i.e. p_5/V_3, cf. Fig. 3) for the transducer structure shown in Fig. 4a and c, over a frequency range up to 350 kHz, calculated using the *FEMP* model (blue thick lines) (Approach B, cf. Sections 2.3 and 3.3).

For comparison, corresponding calculations have been made using the Mason type 1D model for the transducers, combined with the plane-piston-in-infinite-rigid-baffle model for the sound propagation in the gas between the transducers (Approach A, cf. Section 2.3). These are also shown in Fig. 6, using thin lines. Note that since today there is no useful analytical model available for the piezoelectric element's radial modes describing the effects of front layer, backing and radiation load, a Mason type thickness-extensional (TE) mode model was used to model the transducer vibration in the frequency range of the fundamental radial mode (150 kHz). That is, in these 1D simulations the thickness of the piezoelectric element was set to 13 mm (instead of 3 mm), cf. Fig. 4a. Otherwise the transducer and the medium were the same as in the FE simulations (except that shear waves are not accounted for in the Mason model). Use of the TE mode to "describe" the radial mode is of course an incorrect simplification, but still perhaps the only approach available today in terms of 1D modelling.

From Fig. 6 it appears that - as expected - the frequency response and bandwidth of the source sensitivity obtained using Approach A is different from the more correct description Approach B. In Section 4.3 Approach A is used to evaluate diffraction time delay in the transient part of the signal. It is to be expected from Fig. 6 (and also Fig. 8, discussed later) that use of Approach B would provide a different and more correct description of the signals and the transient diffraction time delay. This is planned to be subject of a later study.

4.2 Diffraction time delay results - stationary part of signal

For time detection in the stationary part of the signal, the diffraction time delay can be obtained directly from the calculated phase response of the diffraction correction, H^{dif}. Fig. 7a shows the phase of H^{dif} calculated according to the two approaches *A* and *B* described in Sections 3.2 and 3.3, respectively. The diffraction correction is shown here as a function of distance (for fixed frequency, 150 kHz), in order to evaluate the effect of different path lengths in the USM.

With respect to the "piston results" (thick line), the figure illustrates the well-known effect that the phase of the diffraction correction changes from about 3° (depends on the *ka* number) at the transmitting transducer (z = 0) to nearly 90° in the farfield (at long ranges). That means, in the nearfield, where the waves are nearly plane, the "piston field" is nearly in phase with the "plane wave field". In the farfield, the "piston field" leads the "plane wave field", by up to a quarter of a period.

Fig. 7a also shows that for the transducer example given in Fig. 4, the diffraction time delay correction at 150 kHz is generally larger than for the piston, especially at short ranges. At long ranges the two curves approach 90° phase shift rel. to the plane wave. This is a result of the "bowl-like" vibration of the transducer, cf. the discussion in connection with Fig. 5.

Fig. 7b shows the phase of H^{dif} calculated using Approach *A* (Eq. (8)), for three different piston diameters in a relevant range for actual USM transducers, 12, 20 and 24 mm, and for fixed frequency, 150 kHz. Since the nearfield length increases by increasing transducer diameter, increased diameter means that one needs to go to longer distances to reach the 90° phase difference between the "piston field" and the "plane wave field".

(a)

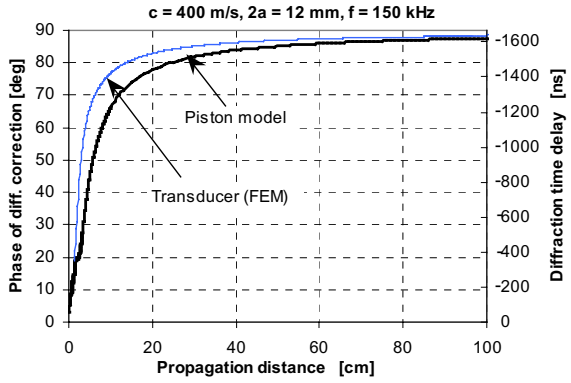

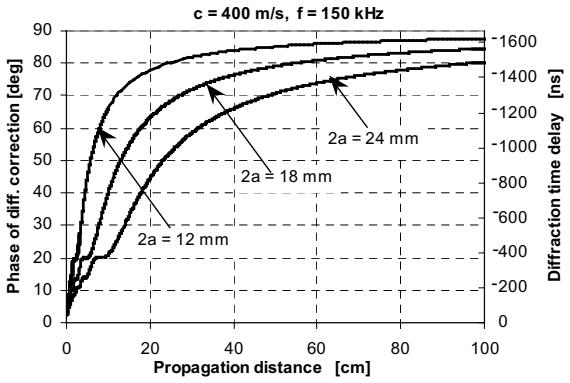

(b)

Fig. 7. Calculated phase of the diffraction correction, shown as a function of distance from the transmitting transducer, at a frequency of 150 kHz. (a) FE calculations for the transducer shown in Fig. 4a and c (Approach B, blue thin line) and William's model for a 12mm diam. plane piston mounted in an infinite rigid baffle (Eq. (8), black thick line, Approach A); (b) William's model for a plane piston mounted in an infinite rigid baffle (Approach A), calculated for piston diameters 12, 20 and 24 mm.

4.3 Diffraction time delay results - transient part of signal

For time detection in the transient part of the signal (e.g. the signal start), the diffraction time delay cannot be obtained directly from the phase response of the diffraction correction H^{dif} (as above), but can be extracted from calculated time signals. Here the *FLOSIM* system model is used for this purpose, cf. Section 3.5.

For calculation of time signals the frequency response of H^{dif} is needed, cf. Eq. 7b. Fig. 8 shows this frequency response (magnitude and phase), for a fixed transducer distance z = 20 cm, calculated according to the two approaches *A* and *B* described in Sections 3.2 and 3.3, respectively.

On an overall scale, the frequency responses of H^{dif} for the transducer and the plane piston shown in Fig. 8 appear to be relatively similar. However, there are differences, such as for the phase responses at very low frequencies, in the 150 kHz range, and above 200 kHz. This is due to the non-piston-like vibration of the transducer, and that the vibration pattern changes with frequency, cf. the discussion in connection with

Fig. 5. Such deviations may be important for the signal form and diffraction time delay both in the transient and stationary parts of the signal. This topic is planned to be subject of a later study.

(a)

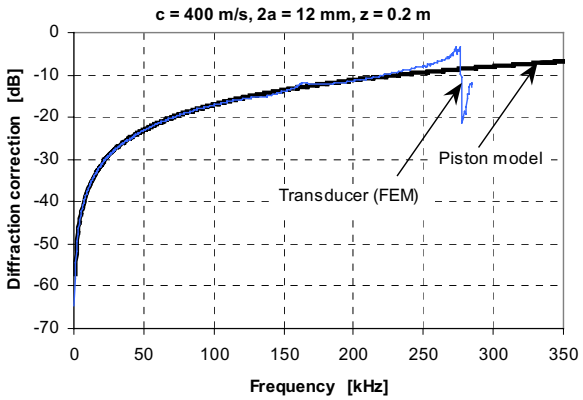

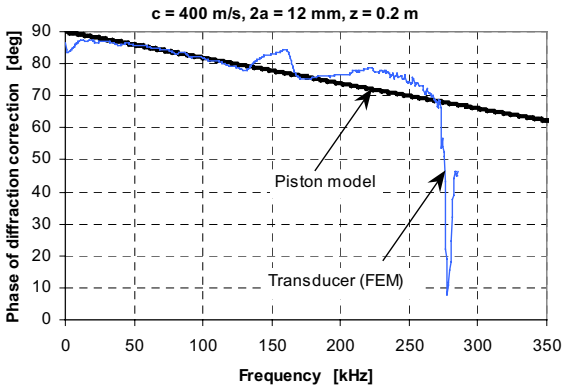

(b)

Fig. 8. Diffraction correction calculated for the transducer shown in Fig. 4a and c (FE calculation, blue thin lines), and for a uniform piston with diameter 12 mm mounted in an infinite rigid baffle (William's model, black thick lines), shown as a function of frequency, at a distance z = 20 cm. (a) magnitude and (b) phase.

For the time signal calculations presented here, Approach A has been used. The following example is considered. The excitation voltage signal $V_0(t)$ is given as a 20 cycle constant amplitude tone burst, starting negative. The internal impedance of the signal generator is Z_S = 1.5 Ω (real). The carrier frequency of the excitation signal is 150 kHz. To simulate the current signal at the output terminals of the receiving transducers (at node 7), an electrical termination impedance of Z_{term} = 1 Ω (real) has been used. For the gas USM simulations, 20 MHz sampling frequency with 8192 sampling points were used. To make the system as simple as possible, and still with sufficient realism to illustrate the main items, no specific electronics or other filtering were used in these simulations.

The diffraction time delay for the time domain signals has been calculated by first simulating the current signal at node 7 using the plane wave propagation model (Eq. (7a)), and next, doing the same calculation using the plane piston model (Eqs. (7b) and (8)). The time difference between corresponding zero crossings in these two signals gives the diffraction time delay for each pair of zero crossings.

Fig. 9 shows the simulated current signal at the output terminals of the receiving transducer using the plane wave propagation model (Eq. (7a)) and the plane piston model (Eqs. (7b) and (8)), at three distances: (a) 0.5 cm, (b) 7 cm and (c) 50 cm. The former distance is well into the nearfield of the transducer, whereas the two latter distances are somewhat and well into the farfield, respectively. For illustration of the diffraction effects in the transient start part of the signal, only the first 7 to 8 out of the 20 cycles of the signal are shown here. The signal becomes nearly stationary at later cycles.

The figure illustrates the well-known effect that the diffraction time delay is nearly zero at signal onset, and becomes negative at later cycles in the signal. That means, at zero crossings within the signal the "piston signal" leads the "plane wave signal", by up to a quarter of a period. This effect may be negligible in the very nearfield of the piston (in which the waves are nearly plane), whereas in the farfield (in which the waves become increasingly spherical with increasing distance) it becomes more pronounced.

Fig. 10 shows the simulated diffraction time delay, i.e. the time difference between corresponding zero crossings in the "piston signal" and the "plane wave signal", as a function of zero crossing number, for the three distances considered in Fig. 9 and some others. It is noted that due to the limited bandwidth of the gas USM transducer, it takes quite a few cycles (about 25 zero crossings) to reach constant diffraction time delay. However, it is also noted that already at the first zero crossing after signal onset the diffraction time delay of this transducer is in the range 70-80 % of the maximum diffraction time delay of the signal (the stationary part value), for a given distance. In general this depends on the transducer's frequency

response and bandwidth, however, and should be addressed in relation to whether time detection is made in the transient start of the signal, or in the stationary part.

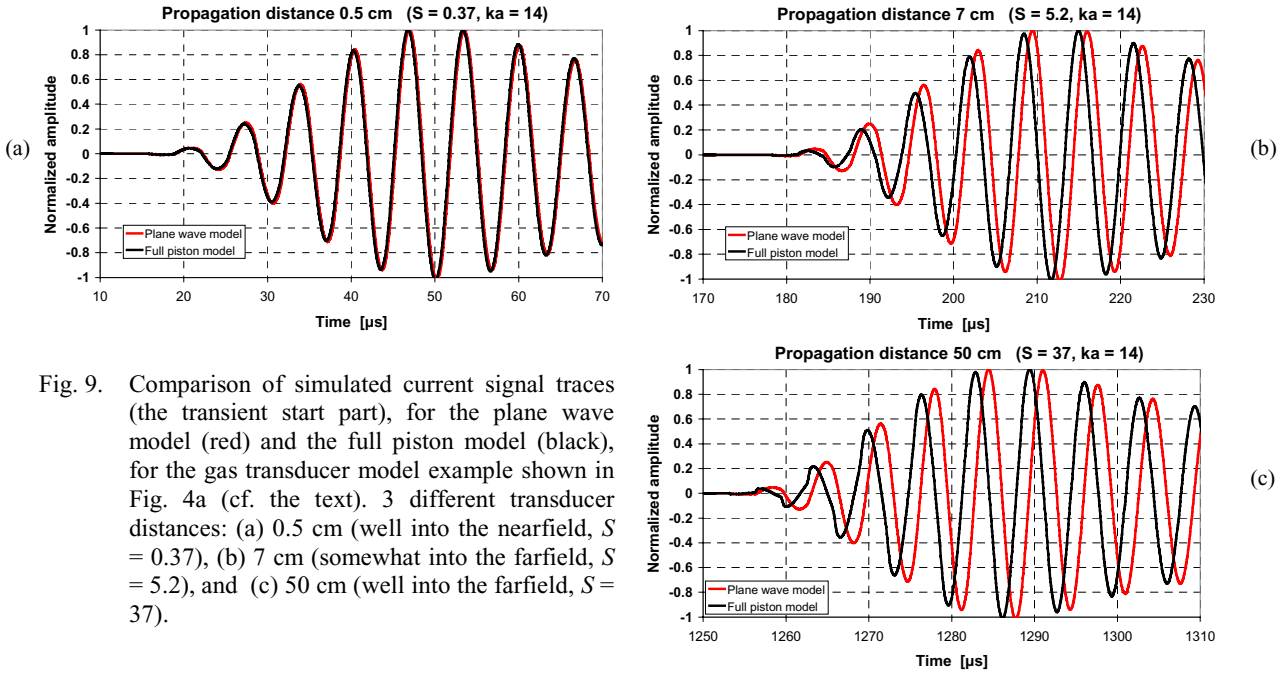

Fig. 9. Comparison of simulated current signal traces (the transient start part), for the plane wave model (red) and the full piston model (black), for the gas transducer model example shown in Fig. 4a (cf. the text). 3 different transducer distances: (a) 0.5 cm (well into the nearfield, S = 0.37), (b) 7 cm (somewhat into the farfield, S = 5.2), and (c) 50 cm (well into the farfield, S = 37).

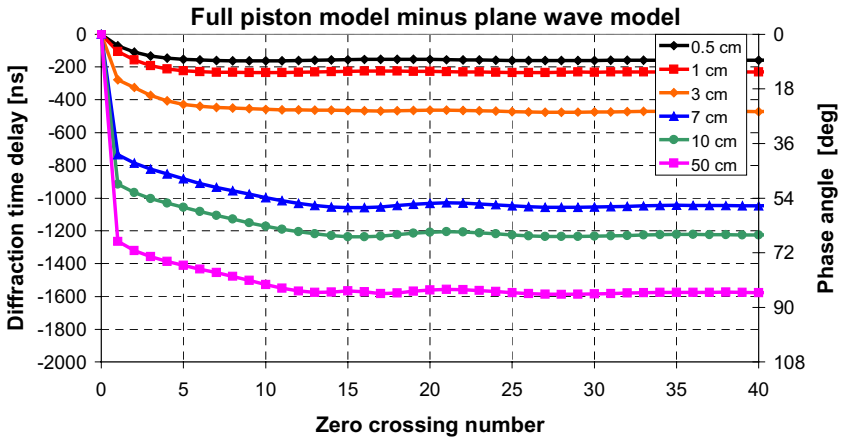

Fig. 10. Simulated diffraction time delay in the transient to the stationary parts of the signal, for the gas transducer model example shown in Fig. 4a (cf. the text), calculated from simulated signal traces, including those shown in Fig. 9. (Transducer distances z = 0.5, 1, 3, 7, 10 and 50 cm.)

4.4 Consequences for USMs

The question then arises whether diffraction time delay values as illustrated in Fig. 10 (up to a quarter of a signal cycle, 1.67 µs) have significant consequences for the USM accuracy, in field operation. This appears to be very dependent on the accuracy requirements, the meter size, the actual "dry calibration" method used for the USM in question, and *how* it is being used (e.g. choice of transducer distances).

To examine this question, calculations using Eqs. (1) have been made first with the correct transit times for the USM size in question, and next with errors added to these transit times. For each path in the USM, the transit time error added is the diffraction time delay of the stationary part of the signal (a negative

number), for the path length in question, cf. Fig. 10. The meter was a 4-path USM with Gauss-Jacobi integration [59] and 45° inclination angles. This procedure was repeated for a range of USM diameters.

The consequences for the USM error after use of the various "dry calibration" methods discussed in Section 2.2, are analyzed in the following. Note that here, only errors due to diffraction effects are considered, - all other sources of error (distance measurement, temperature control in "dry calibration", etc.) have been neglected here.

Sound velocity "dry calibration" method. First, consider the example that "dry calibration" has been made using the "sound velocity method" [1], in a dedicated test cell, at a given transducer distance, z_{dry}. As explained in Section 2.2, correction for diffraction time delay should ideally be made for path lengths other than this distance. Fig. 11a shows the calculated error made by not doing such correction, for meter diameters in the range 100 to 600 mm (4" to 24" meters), for some "dry calibration" distances in the range z_{dry} = 10 - 100 cm, and for transducer diameter 20 mm. Significant meter errors are observed; from 0.1 % for 24" meters up to 0.6 % for 4" meters, depending on z_{dry}.

Similarly, Fig. 11b shows the corresponding error for the VOS reading of the USM. Significant errors are observed also for this measurement if diffraction time delay has not been accounted for or handled; - from about 0.25 m/s (0.06 %) for 24" meters up to about 1.45 m/s (0.36 %) for 4" meters, depending on z_{dry}.

Next, consider the example that "dry calibration" has been made using the "sound velocity method" [1], this time in the actual USM meter body (spoolpiece), i.e. at the actual transducer distances of the meter. Fig.12a shows the calculated error made by not correcting for diffraction effects, for the volumetric flow rate. In this case relatively small meter errors up to 0.05 % (for 4" meters) are found. Also for the VOS reading relatively small errors are found, up to 0.1 m/s (0.025 %) for 4" meters, cf. Fig. 12b. This is the effect on diffraction by changing gas, from nitrogen (c = 350 m/s) to natural gas (c = 400 m/s).

(a)

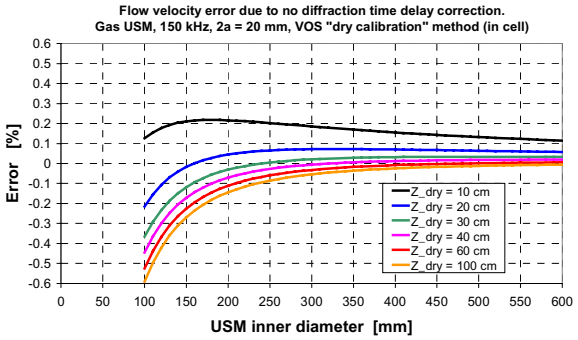

(b)

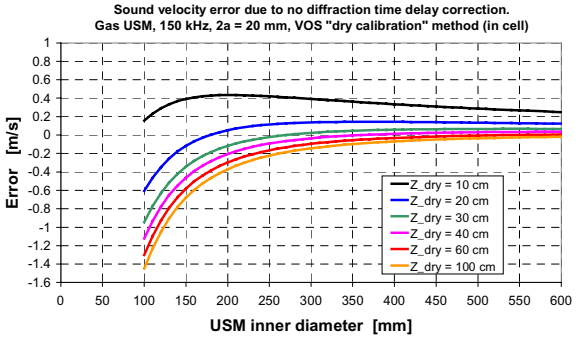

Fig. 11. Simulated error due to no diffraction time delay correction for gas USMs, with respect to (a) flow velocity, and (b) sound velocity. Sound velocity "dry calibration" method (in cell). Transducer diameter = 20 mm.

(a)

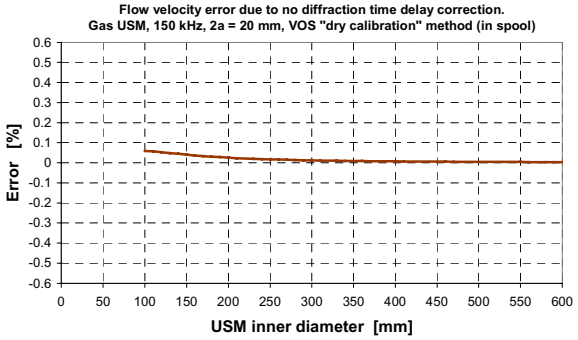

(b)

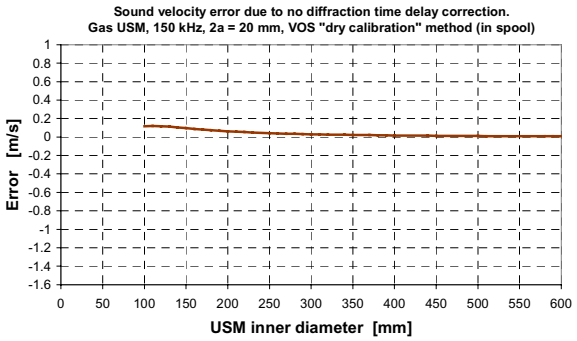

Fig. 12. Simulated error due to no diffraction time delay correction for gas USMs, with respect to (a) flow velocity, and (b) sound velocity. Sound velocity "dry calibration" method (in USM). Transducer diameter = 20 mm.

Two-distance "dry calibration" method. Secondly, consider the example that "dry calibration" has been made using the "two-distance method" [1], at two transducer distances, z_{dry1} and z_{dry2}. As explained in Section 2.2, correction for diffraction time delay should ideally be used. Fig. 13a shows the calculated error made by not doing such correction, for meter diameters in the range 100 to 600 mm (4" to 24" meters), for some arbitrarily chosen combinations of "dry calibration" distances (z_{dry1} and z_{dry2}) in the range 10 - 100 cm, and for transducer diameter 20 mm. Significant meter errors are observed; from 0.18 % for 24" meters up to 0.47 % for 4" meters, depending on the chosen combination of z_{dry1} and z_{dry2}. Errors up to 0.56 % have been found using other distance combinations (e.g. 10 and 15 cm).

Similarly, Fig. 13b shows the corresponding error for the VOS reading of the gas USM. Significant errors are observed also for this measurement if diffraction time delay has not been accounted for or handled; - from about 0.4 m/s (0.1 %) for 24" meters up to about 1.1 m/s (0.28 %) for 4" meters, depending on the chosen combination of z_{dry1} and z_{dry2}.

(a)

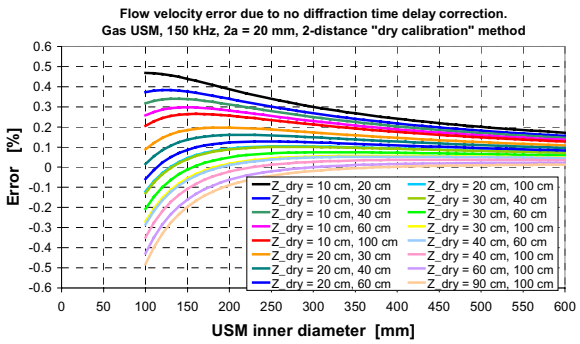

(b)

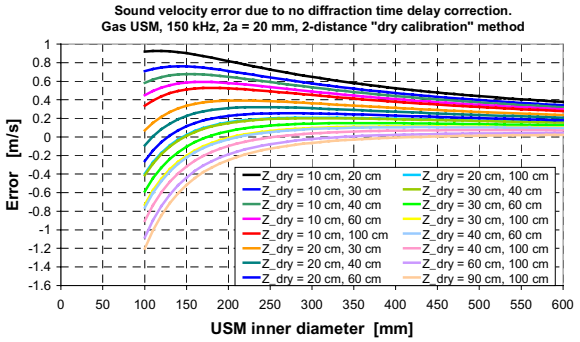

Fig. 13. Simulated error due to no diffraction time delay correction for gas USMs, with respect to (a) flow velocity, and (b) sound velocity. Two-distance "dry calibration" method. Transducer diameter = 20 mm.

Acoustic reflector and transducer reflection "dry calibration" methods. Thirdly, consider the example that "dry calibration" has been made either using the "acoustic reflector method" or the "transducer reflection method". As explained in Section 2.2, neither of these methods account for diffraction time delay, which then needs to be corrected for separately.

Fig. 14a shows the calculated error for the flow velocity reading of the gas USM if diffraction time delay has not been accounted for or handled in the meter, for meter diameters in the range 100 to 600 mm (4" to 24" meters), and for transducer diameter 20 mm. Significant meter errors are observed; from 0.17 % for 24" meters up to 0.47 % for 4" meters.

(a)

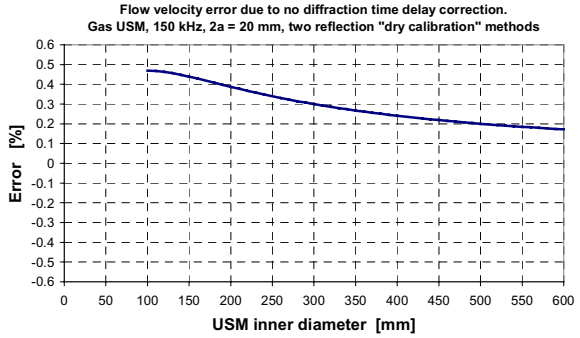

(b)

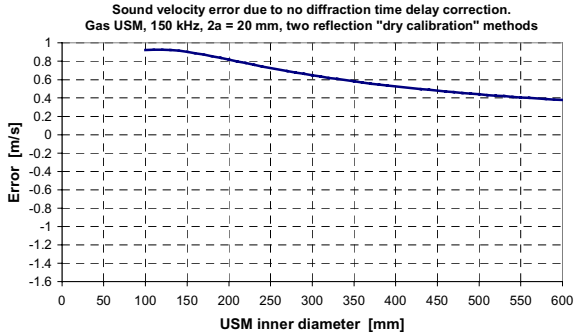

Fig. 14. Simulated error due to no diffraction time delay correction for gas USMs, with respect to (a) flow velocity, and (b) sound velocity. Applies to the following two "dry calibration" methods: the acoustic reflector method, and the transducer reflection method. Transducer diameter = 20 mm.

Similarly, Fig. 14b shows the corresponding error for the VOS reading of the gas USM. Significant errors are observed also for this measurement if diffraction time delay has not been accounted for or handled; - from about 0.4 m/s (0.10 %) for 24" meters up to about 0.9 m/s (0.22 %) for 4" meters.

4.5 Results from flow calibration of a USM

To evaluate the effect of diffraction correction using real USM measurement data, Fig. 15 shows results from flow testing of the FMC Kongsberg Metering gas flow meter MPU 1200 [60] at Statoil's flow calibration laboratory K-Lab in 1999, for the measured flow velocity (Fig. 15a), the sound velocity (Fig. 15b) and the gas density (calculated from the measured sound velocity) (Fig. 15c). The meter under test was a 6" USM, under test conditions of 32 - 86 bar pressure, temperatures 31 - 51 ^{o}C and flow velocities 5 - 20 m/s. For this flow meter test, a "dry calibration" method had been used in which the diffraction time delay was not a part of the measured time delay correction.

First, the meter was flow tested with the diffraction time delay correction "turned off" in the meter software. This resulted in over-readings of the flow velocity (in the range 0.4 - 1.7 %, cf. Fig. 15a) and the sound velocity (in the range 0.9 - 1.2 m/s, Fig. 15b), and a corresponding under-reading of the density (in the range 0.35 - 0.5 %, Fig. 15c).

Next, a new flow testing run was made, this time with the diffraction time delay correction "turned on" in the meter software. The diffraction time delay for the individual paths were calculated according to the piston model described above, with values in a range close to 1.4 µs. This resulted in significant improvements of the meter readings. The flow velocity reading deviations were now in the range -0.2 to 1.1 % (Fig. 15a), the sound velocity reading uncertainties in the range -0.3 to 0.4 m/s (Fig. 15b), and the density reading uncertainties in the range -0.05 to 0.15 % (Fig. 15c).

(a)

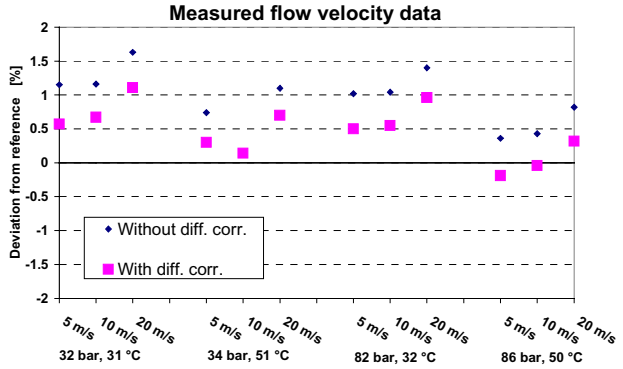

(b)

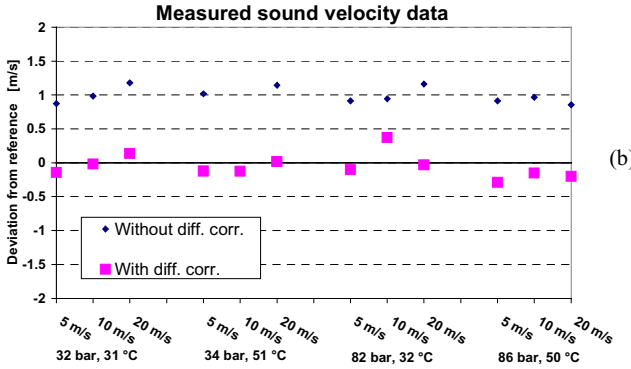

(c)

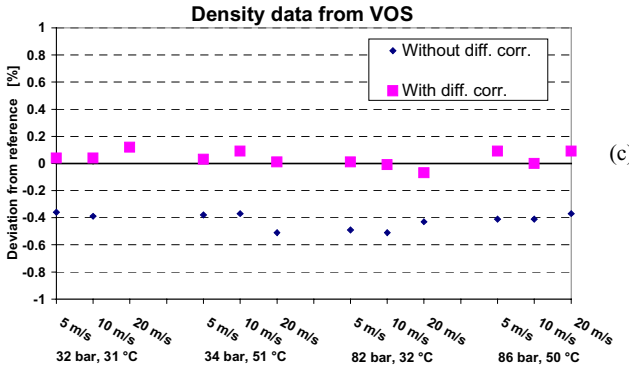

Fig. 15. Results from flow testing of the FMC Kongsberg Metering gas flow meter MPU 1200 at Statoil's flow calibration laboratory K-Lab in 1999, with and without use of diffraction time delay correction. (a) flow velocity, (b) sound velocity, VOS, and (c) gas density (calculated from the measured VOS [13,15]).

The shifts in the flow and sound velocities by activating the diffraction time delay correction in software were typically about 0.5 % and 1 m/s, respectively. It is interesting to note that these measured shift figures are relatively close to the calculated shift figures of a 6" (150 mm) USM shown in Fig. 14, which

are about 0.45 % and 0.9 m/s respectively. Very close agreement is not to be expected, however, since the path configurations, integration methods and signal frequencies of the MPU 1200 and the USMs used to calculate Fig. 14, are different.

5. DISCUSSION, CHALLENGES AND FUTURE DEVELOPMENTS

The diffraction time delay results shown in Sections 4.2-4.5 are discussed in the following, with emphasis on consequences for USM accuracy in flow calibration and field operation, as a basis for the conclusions stated in Section 6.

The results of the present work indicate that when high USM accuracy is in question, diffraction effects can result in a significant metering error after "dry calibration", especially for small-size meters (4"-12"), if not corrected for in the meter. This is so for all of the four "dry calibration" methods discussed here, cf. the example calculations shown in Figs. 11-14. For a 6" meter, for example, and for a 20 mm diam. transducer, Figs. 11-14 indicate that errors due to diffraction of up to 0.45 % and 0.9 m/s (0.22 %) may be experienced for the volumetric flow rate and VOS readings, respectively. However, the errors depend largely on *how* the chosen "dry calibration" method is being used (choice of transducer distances), meter size, and also on several other parameters (cf. Section 3.4).

The example calculations shown in Figs. 11-14 are valid under the assumption of a plane piston vibration of the transducer. As is well known, real transducer vibrations are normally not piston-like (cf. e.g. Figs. 4-8). The finite element calculations shown in Fig. 7a indicate that the error due to diffraction effects may be of the same order of magnitude as indicated in Figs. 11-14 also for real transducers, although the error will definitely depend on the actual vibration pattern of the transducer, at the operational frequency of the USM. The FEM results shown in Figs. 5-8 are considered to represent an important step towards more precise evaluation of diffraction effects and their consequences for real transducers, using finite element modelling of piezoelectric transducers and their radiation.

The example calculations shown in Figs. 11-14 apply to time detection in the stationary part of the signal. Fig. 10 shows that for time detection in the start of the signal (one or several of the first cycles), the situation is to a large extent the same (however, with somewhat smaller diffraction time delay, 20-30 %), and correspondingly smaller metering errors). The results have been obtained within the limitations of Approach A used in Section 4.3 (William's model for a plane piston). In future work such analysis of diffraction effects on time signals may be made for real transducers, e.g. using finite element modelling. Work is today underway in this respect [57], cf. Approach B described in Sections 2.3 and 3.3.

In addition to the factors discussed above, there adds the complication that the transducer time delay and the diffraction time delay may depend on pressure (P), temperature (T), gas composition and flow velocity (beam drift) [27].

For gas meters, this may be particularly important. Gas transducers typically involve matching layers made of polymer materials (epoxy, plastics, etc.), which generally make the transducer time delay temperature dependent, and possibly also pressure dependent. Moreover, the sound velocity of the natural gas changes with P and T, and the vibration of the transducer front may also change with T (and P). As a consequence, the diffraction time delay may be T (and P) dependent.

This may influence on the gas meter accuracy. Due to limitations with actual flow calibration laboratories, the flow calibration conditions may be significantly different from the actual field conditions at which the meter shall operate, such as with respect to P and T. In practice, flow calibration at pressures higher than 50 bar may be difficult to achieve, and the temperature at calibration may typically be e.g. 10 ^{o}C. If the operational conditions are significantly different from the flow calibration conditions, and if the shifts in time delays are not corrected for, an error in the meter reading may be introduced.

In further work on evaluation of the consequences of diffraction effects on the USM accuracy, several factors which have not been addressed here should be considered, such as:

- The influence of temperature (T) and pressure (P) on diffraction time delay (transducer vibration and gas sound velocity effects, from flow calibration to field operation).
- The influence of real transducer vibration, frequency response and bandwidth on diffraction time delay, in the transient part (start) and the stationary part of the signal.
- Beam drift (flow) effects.
- Effects of transducer port geometry (signal interference due to acoustic reflections).

Recent developments in finite element modelling of ultrasonic measurement systems (cf. e.g. [57]) have enabled possibilities for analysis of several of these factors using more accurate modelling of the transducers and the resulting sound wave propagation.. By use of a well proven finite element model, both more realistic (non-uniform) front surface vibration and the associated sound propagation in the fluid, including interference from transducer side-radiation, as well as realistic transducer frequency response and bandwidth, can be described, and e.g. the consequences for the diffraction time delay in the transient and stationary parts of the signal evaluated.

There are however definitely challenges related to use of models such as *FLOSIM* and *FEMP* for applications as discussed above. Some of the ongoing work is concentrated on: (a) ensuring sufficiently reliable and accurate results for the FE calculated functions to be used in *FLOSIM*, with respect to magnitude and phase responses, (b) ensuring correct physical interpretations and uses of the FEM results, (c) ensuring accurate FEM based transducer diffraction correction calculations, (d) performing comparisons with more traditional models for the transducers and the sound field propagation, and (e) comparisons with experimental results.

In the comparisons with experimental results, the available data for the material constants become crucial. For piezoelectric materials, for example, only typical data with a low accuracy (5-20 %) may be available from the manufacturer, at best. Such data are obtained using standardized measurement methods (cf. e.g. [61]). However, the standardized methods have been shown to be physically incorrect because only one-dimensional models are used in the analysis of the measurements, resulting in errors which can be up to several percent [62]. Practical work shows that adjusted values of the material constants may have to be used in the simulations. That has been done in the simulations shown in Figs. 4-9.

Also for non-piezoelectric materials the availability of reliable material data may be a challenge, including material data as a function of temperature T (e.g. to evaluate transducer and diffraction time delays as a function of T).

6. CONCLUSIONS

USM technology for custody transfer volumetric metering of natural gas are of significant and increasing interest for the petroleum industry. This technology is constantly being developed towards more accurate, reliable and cost effective meters. In parallel, there are developments towards measurement of additional quantities (e.g. energy and mass metering of gas). Such developments imply increased requirements to correct and accurate signal analysis and corrections, where also improved treatment of physical, acoustical effects is important.

In the present work, it has been shown that after “dry calibration” of a USM, there may still be an error left in the USM reading due to diffraction effects, if such effects are not being corrected for. This is so for all of the four “dry calibration” methods discussed here. This error may be significant, depending on the

accuracy requirements, the meter size, the choice of "dry calibration" method being used for the meter, and *how* this method is being used. This has been demonstrated in flow calibration and by simulations.

It is well known that for the volumetric flow rate measurement, errors left after "dry calibration" (due to systematic effects such as e.g. diffraction, cf. Fig. 11-14) can be reduced (or even eliminated in some cases) by flow calibration. On the other hand, it is also well known that correction factors established in USM flow calibration may in practice not be "perfect", in the meaning that errors may not be fully eliminated (cf. e.g. [30,31]). Besides, the AGA-9 report [1, Chapter 5] requires that in flow calibration the USM shall "meet the minimum requirements before the application of any calibration-factor adjustment" (i.e., 1.4 % in the low velocity range, and 0.7-1.0 % elsewhere), to "ensure that a major flaw in the meter is not masked by a large calibration-factor adjustment". Thirdly, if the temperature T (and pressure P) are significantly different from flow calibration to field operation, systematic diffraction time delay effects may be introduced.

For the VOS measurement, used in USM diagnostics and extended applications such as mass and energy flow rate metering, flow calibration does *not* reduce errors left after "dry calibration" (due to systematic effects such as e.g. diffraction, cf. Figs. 11-14). In USM diagnostics, for example, VOS is compared between paths. As diffraction effects will act differently on paths of different length, the use of diffraction time delay correction can help to reduce the VOS spread between paths, and thus improve the VOS method as a tool for USM diagnostics.

For use of VOS in mass and energy flow rate metering, the errors due to diffraction may be of an order of magnitude where control with diffraction effects will be important.

For reasons as discussed above, treatment of diffraction effects may be highly recommended, especially for small-size meters (4"-12"). That means, use of diffraction time delay correction in "dry calibration", in flow calibration (accounting for actual path lengths), and in field operation (accounting for P and T effects).

Such correction may be done conveniently in USM software. Methods for developing and implementing diffraction time delay correction algorithms in USM software are available today. The cases of time detection in the transient (start) or the stationary (middle) parts of the signal need to be treated differently, but the available methods cover both cases.

It is worth noting that even an idealized and simplified description of diffraction effects based on the plane piston model may in many cases reduce USM errors due to diffraction to an acceptable level. Such an approach has been demonstrated here to result in significant improvement of the USM accuracy in flow calibration, cf. Fig. 15.

More refined, powerful and accurate models are also available today. Recent developments in finite element modelling of ultrasonic measurement systems have enabled possibilities for analysis of several of the influencing factors using much more accurate modelling of the transducers and the radiated sound field. Individual transducer characteristics, such as the vibration pattern and change of this pattern with frequency, can be accounted for in the diffraction correction.

In perspective, it is important to be aware that the results presented here do not question the basic soundness and reliability of the USM method. The diffraction effects discussed here become important essentially when (a) high accuracy in the volumetric flow rate reading is necessary, and (b) for extended functionality of USMs (use of the measured VOS to calculate the mass and energy flow rates). Control of diffraction effects become especially important for the VOS measurement, for which possible systematic effects (errors) are *not* being eliminated or reduced by flow calibrating the meter.

Methods to achieve improved control with systematic transit time effects such as due to diffraction, etc., have been described here. The results of the present work are expected to provide a basis to further improve today's USM technology towards higher accuracy, control, reliability and functionality.

ACKNOWLEDGEMENTS

The present work has been supported by The Research Council of Norway (NFR), under a 4-year strategic institute programme "Ultrasonic technology for improved exploitation of petroleum resources" (2003-06). In addition, the work has evolved from project cooperation over time related to USM fiscal metering of gas and oil (custody transfer, sales and allocation metering), involving several partners: The Norwegian Society for Oil and Gas Measurement (NFOGM), the Norwegian Petroleum Directorate (NPD), GERG (Groupe Européen de Reserches Gazières), FMC Kongsberg Metering, FMC Smith Meter (USA), Roxar Flow Measurement, Statoil, Norsk Hydro and ConocoPhillips. FMC Kongsberg Metering is acknowledged for permission to use the MPU 1200 flow calibration results shown in Fig. 15.

REFERENCES

[1] **AGA-9**, "Measurement of gas by ultrasonic meters", A.G.A. Report no. 9, American Gas Association, Transmission Measurement Committee (June 1998).

[2] "Regulations relating to measurement of petroleum for fiscal purposes and for calculation of CO_2 tax", Norwegian Petroleum Directorate (NPD), Stavanger, Norway (November 2001).

[3] **Lansing, J.:** "Smart monitoring and diagnostics for ultrasonic gas meters", *Proc. of 18th International North Sea Flow Measurement Workshop, Gleneagles, Scotland, 24-27 October 2000.*

[4] **Smalling, J.W., Braswell, L. D. and Lynnworth, L. C.:** "Apparatus and methods for measuring fluid flow parameters." US patent no. 4,596,133, dated June 24, 1986 (filed July 29, 1983).

[5] **Smalling, J.W., Braswell, L. D., Lynnworth, L. C. and Russell Wallace, D.:** "Flare gas ultrasonic flow meter", *Proc. of 39th Annual Symp. on Instrum. for the Process Industries, January 17-20, 1984*, pp. 27-38.

[6] **Lygre, A.:** *"*A method for estimating density, isentropic exponent and molecular weigth of natural gas at low pressures", CMR Report CMI 871412-1, Christian Michelsen Research, Norway (1988) (Confidential).

[7] **Tjomsland, T. and Frøysa, K.-E.:** "Calculation of natural gas density from sound velocity. Description of theory and algorithms implemented in the Deca code", CMR report no. CMR-97-F10015, Christian Michelsen Research AS, Bergen, Norway (June 1997) (Confidential).

[8] **Watson, J.:** "A review of important gas flow measurement parameters." *Proc. of Practical Developments in Gas Flow Metering, One Day seminar - 7 April 1998*, National Eng. Lab. (NEL), East Kilbride, Scotland (1998).

[9] **Beecroft, D.:** "Is a wet gas (multiphase) mass flow meter just a pipe dream?", *Proc. of 16th International North Sea Flow Measurement Workshop, Gleneagles Hotel, Perthshire, Scotland, 26-29 October 1998.*

[10] **Frøysa, K.-E., Furset, H. and Baker, A. C.:** "Density and ultrasonic velocity calculations for natural gas. Sensitivity analysis of DeCa", CMR report no. CMR-98-F10002, Christian Michelsen Research AS, Bergen, Norway (December 1998) (Confidential).

[11] **Nesse, Ø. and Frøysa, K.-E.:** "Ultrasonic natural gas density estimation. Sound velocity measurements in nitrogen", CMR-98-F10026, Christian Michelsen Research AS, Bergen, Norway (Dec. 1998) (Confidential).

[12] **Baker, A. C., Frøysa, K.-E. and Midttun, Ø.:** "*NATSIM* user guide. A program for calculating compressibility, sound speed, density, heat capacity and calorific value of gases," CMR-TN98-F10030, Christian Michelsen Research AS, Bergen, Norway (Dec. 1998) (Confidential.)

[13] **Lunde, P., Frøysa, K.-E., Fossdal, J. B. and Heistad, T.:** "Functional enhancements within ultrasonic gas flow measurement", Proc. of *17th Intern. North Sea Flow Measurem. Workshop, Oslo, Norway, 25-28 Oct. 1999*.

[14] **Lunde, P. and Frøysa, K.-E.:** "Mass and energy measurement of gas using ultrasonic flow meters". *Proc. of the 25th Scandinavian Symposium on Physical Acoustics, Ustaoset, Norway, 27-30 January 2002.* Rep. No. 420103, Norwegian University of Science and Technology, Trondheim (June 2002). (CD issue).

[15] **Haruta, M., Uekuri, K. and Kiuchi, Y.:** "Continuous measurement of calorific value of natural gas." Proc. of *Symposium on Natural Gas Energy Measurement, Chicago, 1986*, p. 401-427.

[16] **Lueptow, R. M. and Phillips, S.:** "Acoustic sensor for determining combustion properties of natural gas." Meas. Sci. Technol. 5, 1375-1381 (1994).

[17] **Tjomsland, T. and Frøysa, K.-E.:** "Calorific value of natural gas. Possible determination from temperature, pressure and sound velocity", CMR-96-F10022, Chr. Michelsen Research AS, Bergen (Dec. 1996) (Confident.)
[18] **Baker, A. C. and Frøysa, K.-E.:** "A technique for the calculation of the energy content of a natural gas", CMR-97-F10028, Christian Michelsen Research AS, Bergen, Norway (December 1997) (Confidential).
[19] **Baker, A. C. and Frøysa, K.-E.:** "Further work on ENCON", CMR report no. CMR-98-F10029, Christian Michelsen Research AS, Bergen, Norway (December 1998) (Confidential).
[20] **Morrow, T. D. and Behring, K. A .:** "Energy flow measurement technology, and the promise of reduced operating costs", *Proc. of 4th Intern. Symp. on Fluid Flow Measurem., Denver, Colorado, June 27-30, 1999.*
[21] *Flow Tidings - The Flow Programme Newsletter,* Issue 31, Summer 2001, National Engineering Laboratory (NEL), East Kilbride, Scotland.
[22] Collection of papers and presentations, titled "Energy flow measurement system", dated December 13, 2001. Gasunie Research, Groeningen, the Netherlands.
[23] **S. Vervik,** "Transitt-tidsbestemmelse for ultralyd strømningsmetre. Nullstrømningsforhold". Thesis for the Cand. Scient. degree. Dept. of Physics, Univ. of Bergen. (In Norwegian) (1995).
[24] **M. Kanagasundram,** "Acoustic effects on pulse forming in ultrasound transit time gas flow meters at no flow conditions". Thesis for the Cand. Scient. degree. Dept. of Physics, Univ. of Bergen (1995).
[25] **M. Vestrheim and S. Vervik,** "Transit time determination in a measurement system, with effects of transducers". *Proc. of 1996 IEEE Intern. Ultrason. Symp.* (1996)
[26] **S. Vervik,** "Methods for characterization of gas-coupled ultrasonic sender-receiver measurement systems". Thesis for the Dr. Scient. degree. Dept. of Physics, Univ. of Bergen (2000).
[27] **Lunde, P., Frøysa, K.-E. and Vestrheim, M. (eds.):** "GERG project on ultrasonic gas flow meters, Phase II", GERG TM11 2000, Groupe Européen de Recherches Gazières (VDI Verlag, Düsseldorf, 2000).
[28] **Lunde, P., Frøysa, K.-E. and Vestrheim, M.:** "Challenges for improved accuracy and traceability in ultrasonic fiscal flow metering", *Proc. of 18th Intern. North Sea Flow Measurem. Workshop, Gleneagles, Scotland, 24-27 Oct. 2000.*
[29] **Lunde, P., Frøysa, K.-E. and Vestrheim, M.:** "Transient diffraction effects in ultrasonic flow meters for gas and liquid". *Proc. of 26th Scandinavian Symposium on Physical Acoustics, Ustaoset, Norway, 26-29 January 2003.* Rep. No. 420304, Norwegian University of Science and Technology, Trondheim (June 2003). (CD issue.)
[30] **Lunde, P. and Frøysa, K.-E.:** "Handbook of uncertainty calculations - Ultrasonic fiscal gas metering stations", Norwegian Petroleum Directorate, Norwegian Society for Oil and Gas Measurement (NFOGM), Christian Michelsen Research, Norway (December 2001). ISBN 82-566-1009-3.
[31] **Lunde, P., Frøysa, K.-E., Neumann, S. and Halvorsen, E.:** "Handbook of uncertainty calculations. Ultrasonic fiscal gas metering stations". *Proc. of 20th North Sea Flow Measurement Workshop,* St. Andrews Bay, Scotland, 22-25 October 2002.
[32] **Frøysa, K.-E., Lunde, P. and Vestrheim, M.,** "A ray theory approach to investigate the influence of flow velocity profiles on transit times in ultrasonic flow meters for gas and liquid", *Proc. of 19th International North Sea Flow Measurement Workshop, Kristiansand, Norway, 22-25 October 2001*.
[33] **Hallanger, A., Frøysa, K.-E. and Lunde, P.:** "CFD simulation and installation effects for ultrasonic flow meters in pipes with bends", International Journal of Applied Mechanics and Engineering, **7(**1), 33-64 (2002).
[34] **Angus, S., de Reuck, K.M. og Armstrong, B. (Eds.):** *International Thermodynamic Tables of the Fluid State - Vol. 6. Nitrogen.* International Union of Pure and Applied Chemistry (IUPAC), Chemical data Series No. 20 (Pergamon Press, Oxford 1979).
[35] **Folkestad, T. and Johannessen, A.A.:** "FMU 700 - Fiskal måler ultralyd. Datamaskin", CMR-93-F10004, Christian Michelsen Research AS, Bergen, Norway (July 1993). (Confidential, in Norwegian.)
[36] **A. O. Williams,** "The piston source at high frequencies", J. Acoust. Soc. Am. **23**, 1-6 (1951).
[37] **E. P. Papadakis,** "Correction for diffraction losses in the ultrasonic field of a piston source", J. Acoust. Soc. Am. **31**(2), 150-152 (1959).
[38] **H. J. McSkimin,** "Experimental study of the effect of diffraction on velocity of propagation of high-frequency waves", J. Acoust. Soc. Am. **32**(11), 1401-1404 (1960).
[39] **E. P. Papadakis,** "Ultrasonic phase velocity by the pulse-echo-overlap method incorporating diffraction phase corrections", J. Acoust. Soc. Am. **42**(5), 1045-1051 (1967).
[40] **M. B. Gitis and A. S. Khimunin,** "Diffraction effects in ultrasonic measurements" (review), Sov. Phys. Acoust. **14**(4), 413-431 (1969).
[41] **E. P. Papadakis,** "Ultrasonic diffraction loss and phase change for broad-band pulses", J. Acoust. Soc. Am. **52**(3, Pt.2), 847-849 (1972).
[42] **A. S. Khimunin,** "Numerical calculation of the diffraction corrections for the precise measurement of ultrasonic absorption", Acustica **27**(4), 173-181 (1972).
[43] **A. S. Khimunin,** "Numerical calculation of the diffraction corrections for the precise measurement of ultrasound phase velocity", Acustica **32**, 192-200 (1975).

[44] **T. L. Rhyne,** "Radiation coupling of a disk to a plane and back or a disk to a disk: An exact solution", J. Acoust. Soc. Am. **61**(2), 318-324 (1977).
[45] **A. S. Khimunin,** "Ultrasonic parameter measurements incorporating exact diffraction corrections", Acustica **39**, 87-95 (1978).
[46] **J. A. Harrison, G. N. Cook-Martin, and R. E. Challis,** "Radiation coupling between two coaxial disks of different diameter: An exact solution and detailed experimental verification", J. Acoust. Soc. Am. **76**(4), 1009-1022 (1984).
[47] **A. S. Khimunin and E. A. Lvova,** "Time-dependent average pressure on the receiver in a circular transducer system", Acustica **56**, 91-104 (1984).
[48] **D. Cassereau, D. Guyomar, and M. Fink,** "Time deconvolution of diffraction effects – Application to calibration and prediction of transducer waveforms", J. Acoust. Soc. Am. **84**(3), 1073-1085 (1988).
[49] **T. Imamura,** "Deformation of ultrasonic pulse with diffraction", Ultrasonics **37**, 71-78 (1999).
[50] **R. Kazys et. al.,** "Evaluation of diffraction errors in precise pulse-echo measurements of ultrasound velocity in chambers with waveguide", Ultrasonics **40**, 853-858 (2002).
[51] **Lunde, P. and Vestrheim, M.:** "Piezoelectric Transducer Modelling. Thickness Mode Vibration." CMI Report No. CMI-91-A10003, Chr. Michelsen Institute, Bergen (December 1991).
[52] **Kinsler, L.E. og Frey, A.R.:** *Fundamentals of Acoustics*, 2nd. ed. (J. Wiley and Sons, 1962).
[53] **A. Lygre, M. Vestrheim, P. Lunde, and V. Berge,** "Numerical simulation of ultrasonic flowmeters". *Proc. of Ultrasonics International 1987*, Butterworth Scientific Ltd., Guildford, UK (1987), pp. 196-201.
[54] **J. M. Kocbach, P. Lunde and M. Vestrheim,** "FEMP - Finite element modeling of piezoelectric structures. Theory and verification for piezoceramic disks", Rep. 1999-07, Univ. of Bergen, Dept. of Physics, 1999.
[55] **J. M. Kocbach,** "Finite element modeling of ultrasonic piezoelectric transducers. Influence of geometry and material parameters on vibration, response functions and radiated field", Dr. Scient. thesis, Univ. of Bergen, Dept. of Physics, Bergen, Norway, Sept. 2000.
[56] **J. M. Kocbach, P. Lunde and M. Vestrheim,** "Resonance frequency spectra with convergence tests for piezoceramic disks using the Finite Element Method", *Acustica*, 87, 271-285, 2001.
[57] **Lunde, P, Kippersund, R.A. and Vestrheim, M.:** "Signal modelling using the *FLOSIM* system model in ultrasonic instrumentation for industrial applications", *Proc. of NORSIG 2003, Norwegian Symposium on Signal Processing 2003*, Bergen, Norway, October 2-4, 2003.
[58] "Piezoelectric ceramics", Product and data brochure, Ferroperm, Denmark (2002).
[59] **Abromowitz, M. and Stegun, I.A.:** *Handbook of mathematical functions*, Applied Mathematics Series, Vol. 55 (National Bureau of Standards, Washington D.C., 1964). Reprint by Dover Public., Inc., New York, May 1968.
[60] "MPU 1200 ultrasonic gas flow meter", Sales brochure, FMC Kongsberg Metering, Kongsberg, Norway (2000).
[61] "IEEE standard on piezoelectricity", ANSI/IEEE std. 176-1987, Inst. of Electr. and Electron. Eng., New York, 1988.
[62] **Vestrheim, M. and Fardal, R.:** "Methods for determining constants of piezoelectric ceramic materials", in *Proc. 25th Scand.. Symp. on Phys. Acoustics,* Ustaoset, Norway, 27-30 January, 2002. Scient./Tech. Rep. 420103, Norw. Univ. of Sc. and Techn., June 2002. (CD issue only).